JOURNAL OF AGRICULTURAL AND FOOD CHEMISTRY

ARTICLE

pubs.acs.org/JAFC

A Synthetic Naringenin Derivative, 5-Hydroxy-7, 4′-diacetyloxyflavanone-*N*-phenyl Hydrazone (N101-43), Induces Apoptosis through Up-regulation of Fas/FasL Expression and Inhibition of PI3K/Akt Signaling Pathways in Non-Small-Cell Lung Cancer Cells

Yesol Bak,[†,∥] Heejong Kim,[†,∥] Jeong-Woo Kang,[†] Dong Hun Lee,[†] Man Sub Kim,[†] Yun Sun Park,[†] Jung-Hee Kim,[†] Kang-Yeoun Jung,[§] Yoongho Lim,[†] Jintae Hong,[#] and Do-Young Yoon*[,†]

[†]Department of Bioscience and Biotechnology, Bio/Molecular Informatics Center, Konkuk University, Seoul, Republic of Korea

[§]Department of Biochemical Engineering, College of Engineering, Gangneung-Wonju National University, Gangneung, Republic of Korea

[#]College of Pharmacy and Medical Research Center, Chungbuk National University, Cheongju, Republic of Korea

ABSTRACT: Naringenin, a well-known naturally occurring flavonone, demonstrates cytotoxicity in a variety of human cancer cell lines; its inhibitory effects on tumor growth have spurred interest in its therapeutic application. In this study, naringenin was derivatized to produce more effective small-molecule inhibitors of cancer cell proliferation, and the anticancer effects of its derivative, 5-hydroxy-7,4′-diacetyloxyflavanone-*N*-phenyl hydrazone (N101-43), in non-small-cell lung cancer (NSCLC) cell lines NCI-H460, A549, and NCI-H1299 were investigated. Naringenin itself possesses no cytotoxicity against lung cancer cells. In contrast, N101-43 inhibits proliferation of both NCI-H460 and A549 cell lines; this capacity is lost in p53-lacking NCI-H1299 cells. N101-43 induces apoptosis via sub-G_1 cell-cycle arrest in NCI-H460 and via G_0/G_1 arrest in A549 cells. Expression of apoptosis and cell-cycle regulatory factors is altered: Cyclins A and D1 and phospho-pRb are down-regulated, but expression of CDK inhibitors such as p21, p27, and p53 is enhanced by N101-43 treatment; N101-43 also increases expression levels of the extrinsic death receptor Fas and its binding partner FasL. Furthermore, N101-43 treatment diminishes levels of cell survival factors such as PI3K and p-Akt dose-dependently, and N101-43 additionally induces cleavage of the pro-apoptotic factors caspase-3, caspase-8, and poly ADP-ribose polymerase (PARP). Cumulatively, these investigations show that the naringenin derivative N101-43 induces apoptosis via up-regulation of Fas/FasL expression, activation of caspase cascades, and inhibition of PI3K/Akt survival signaling pathways in NCI-H460 and A549 cells. In conclusion, these data indicate that N101-43 may have potential as an anticancer agent in NSCLC.

KEYWORDS: naringenin derivative, apoptosis, lung cancer, flavonoid

INTRODUCTION

Lung cancer is one of the most common cancers globally and the major cause of cancer deaths, having surpassed breast cancer as the leading cause of cancer mortality in women in 1987; by 2002 it was predicted to account for approximately 25% of all female deaths from cancer.[1] The high incidence of mortality is a result of the difficulty of early diagnosis and lung tumors' elevated potential for local invasion as well as metastasis to distant tissues and organs.[2] The most predominant forms of lung cancer are non-small-cell lung cancer (NSCLC), accounting for about 85% of cases, and small-cell lung cancer (SCLC), accounting for 15% of cases.[3] In comparison to small-cell carcinomas, NSCLCs are relatively insensitive to chemotherapy. Thus, there is urgent need to improve clinical management of this serious disease.

Apoptosis, or programmed cell death, plays a pivotal role in the normal development and pathology of a wide variety of tissues. It can be easily distinguished from necrosis through its diverse alterations to the cell, including chromatin condensation, DNA fragmentation, cytoplasmic shrinkage, and the formation of apoptotic bodies.[4,5] However, most cancer cells do not undergo apoptosis due to impairment of apoptotic signal transmission.[6] Triggering apoptosis in tumor cells can therefore be an effective strategy in anticancer therapy.

Apoptosis can occur through two mechanisms, the extrinsic death-receptor dependent pathway and a mitochondria-dependent, or intrinsic, pathway.[7,8] The extrinsic pathway is activated by cell-surface ligand-gated death receptors such as the tumor necrosis factor receptor superfamily. The association of specific ligands with the extracellular domains of death receptors triggers receptor trimerization: these ligands include CD95L/FasL and Apo2L/TRAIL, which bind their respective cognate receptors CD95/Fas and DR4/DR5.[9,10] The Fas-associated death domain (FADD) recruits caspase-8 to the Fas receptor to form the death-inducing signaling complex (DISC).[11] Oligomerization of caspase-8 upon DISC formation triggers its activation concomitant with that of downstream effectors such as caspase-3.[10,12] Intrinsic apoptosis is initiated by disparate extracellular and intracellular death stimuli: in the mitochondrial apoptosis pathway, caspase

Received: May 10, 2011
Revised: August 18, 2011
Accepted: August 30, 2011
Published: August 30, 2011

activation stems from permeabilization of the outer mitochondrial membrane by pro-apoptotic factors in the Bcl family and is regulated by Bcl-2 and mitochondrial lipids. Mitochondrial release of cytochrome *c* directly triggers caspase-3 activation through formation of the cytochrome *c*/Apaf-1/caspase-9-containing apoptosome complex. Caspase-3 then cleaves cellular targets to promote programmed cell death.[10,13]

The phosphatidylinositol 3-kinase (PI3K) signaling pathway plays pivotal roles in the signal transduction of survival in a wide range of cell types including neurons.[14,15] PI3K activates its downstream effector protein Akt/protein kinase B (Akt/PKB) by promoting its phosphorylation at residues serine 473 (Ser473) and threonine 308 (Thr308). Then activated Akt phosphorylates a wide range of substrates, activating anti-apoptotic (survival) factors and inactivating pro-apoptotic factors.[15] Akt down-regulates the activities of glycogen synthase kinases 3α (GSK3α) and 3β (GSK3β) by phosphorylating the former at residue serine 21 (Ser21) and the latter at residue serine 9 (Ser9).[16] GSK3 is a highly evolutionary conserved intracellular serine−threonine kinase that exists as two isoforms, GSK3α and GSK3β, ubiquitously expressed in mammalian tissues.[17] Phosphorylation, and therefore inactivation of GSK3, can be catalyzed by insulin, growth factors, and amino acids throughout the PI3K/Akt, MAPK cascade, protein kinase C (PKC), or cAMP-dependent protein kinase/protein kinase A.[18−20] GSK3 regulates diverse cell functions such as protein synthesis, cell proliferation, cell differentiation, apoptosis, microtubule dynamics, and cell motility.[21]

Plant extracts have begun to receive attention as therapeutic agents in cancer treatment due to their capacity to inhibit tumor growth, angiogenesis, and metastasis with minimal side effects. Flavonoids are plant secondary metabolites often found in fruits, vegetables, and plant-derived beverages or in dietary supplements or herbal remedies.[22] They comprise a diverse group of plant natural products synthesized from phenylpropanoid and acetate-derived precursors and play seminal roles in growth, development, and host defense against microorganisms or pests.[23] In structure, they are low molecular weight polyphenols with a characteristic 2-phenylbenzo-γ-pyrone structure harboring one or more hydroxyl groups. One of their most obvious features is their ability to quench free radicals via formation of resonance-stabilized phenoxyl radicals,[24] and they can also exhibit antifungal, anti-inflammatory, or antitumor effects.[25] Additionally, they are safe for human consumption and, in some cases, are suggested to be good chemopreventive agents.

Naringenin, a glycone of naringin, is abundant in citrus fruits, grapes, and tomatoes.[26] Naringenin has been discovered to possess activity against uterine, blood, stomach, brain, and lung cancer cell lines[27−30] at doses that do not affect nontransformed cells.[31] Although many studies report these anticancer properties, their precise mechanisms remain unclear in NSCLC. It has been known that naringenin inhibits NF-κB, which is a key transcription factor involved in cancer growth.[32] Therefore, to find a novel derivative showing anticancer activity, we tried to synthesize several naringenin derivatives. The cell viability test for them revealed that several compounds exhibited at least a 20% decrease. Especially, N101-43 including an acetate group and phenylhydrazine showed the best result. As a result, we focused on the N101-43 compound. On the basis of naringenin's putative anticancer activity, we elucidated the effect of the newly synthesized naringenin derivative N101-43 on the growth of NSCLC cells and the intracellular signal transduction pathways that regulate apoptosis. We demonstrate that N101-43 induces apoptosis via up-regulation of death receptor expression, activation of the apoptotic caspase cascade, and inhibition of PI3K/Akt cell survival signaling pathways in NCI-H460 and A549 cells.

MATERIALS AND METHODS

Reagents. CellTiter 96 AQ_{ueous} One solution Cell Proliferation Assay Reagent (MTS) was purchased from Promega (Madison, WI). Hoechst stain solution and propidium iodide (PI) were purchased from Sigma (St. Louis, MO). A pan-caspase inhibitor, Z-VAD-fmk, and a PI3K inhibitor, LY294002, were from R&D Systems (Minneapolis, MN) and Calbiochem (Darmstadt, Germany), respectively.

Synthesis of 5-Hydroxy-7,4′-diacetyloxyflavanone-*N*-phenyl Hydrazone (N101-43). As shown in Figure 1A, N101-43 is a newly synthesized naringenin derivative. Prior synthesis of 5,7,4′-trihydroxy flavanone *N*-phenyl hydrazone (named N101-3) was required for N101-43 synthesis. Naringenin (3.0 g (11.02 mmol)) and phenyl hydrazine (1.3 mL (13.22 mmol)) were dissolved in absolute ethanol (20 mL), and glacial acetic acid (1.0 mL) added. The solution was refluxed on an oil bath for 36 h at 110−120 °C with stirring until a yellow precipitate formed. The precipitate was collected by filtration and washed with water and ethanol. The crude product was purified by flash column chromatography using a gradient solvent system with acetone and chloroform to obtain the desired product, N101-3, as a brown solid (3.18 g (8.78 mmol), 79.7% yield): ^{1}H NMR δ 2.81 (dd, J = 12.09, 16.86 Hz, 1H), 3.27 (dd, J = 2.91, 17.01 Hz, 1H), 5.07 (dd, J = 2.55, 11.7 Hz, 1H), 5.90 (dd, J = 2.4, 20.16 Hz, 2H), 6.81 (d, J = 8.61 Hz, 2H), 6.95 (d, J = 7.71 Hz, 2H), 7.24 (t, J = 7.88, 15.75 Hz, 2H), 7.34 (d, J = 8.61 Hz, 2H), 9.33 (s, 1H), 9.55 (s, 1H), 9.77 (s, 1H), 12.50 (s, 1H); ^{13}C NMR δ 31.8, 75.9, 95.1, 96.5, 98.8, 112.0 (2C), 115.1 (2C), 119.2, 128.1 (2C), 129.3, 130.2 (2C), 144.9, 145.1, 157.5, 157.7, 159.2, 159.7; IR (cm^{-1}) 3433, 2948, 2054, 1639, 1600, 1499, 1250, 1250, 1154, 1055, 1032, 1019; HRFABMS calcd for $C_{21}H_{18}N_2O_4$ $(M + Na)^+$ 385.1164, found 385.1160. Next, to a solution of N101-3 (0.2 g (0.55 mmol)) in THF (15 mL) was added Et_3N (0.3 mL (2.21 mmol)) under argon gas. After 10 min of stirring at room temperature, acetyl chloride (0.1 mL (1.21 mmol)) was slowly added. After a further 10 min, when thin-layer chromatography demonstrated complete disappearance of the starting material, distilled water was used to quench the reaction. The crude product was purified by flash column chromatography using a gradient solvent system with acetone and chloroform to obtain the desired product, N101-43, as a white solid (0.22 g (0.50 mmol), 91.3% yield): ^{1}H NMR δ 2.31 (d, J = 13.2 Hz, 6H), 2.67 (dd, J = 12.45, 16.47 Hz, 1H), 3.15 (dd, J = 3.3, 16.5 Hz, 1H), 5.14 (dd, J = 2.94, 12.09 Hz, 1H), 6.32 (dd, J = 2.19, 19.41 Hz, 2H), 6.93−7.00 (m, 3H), 7.14−7.19 (m, 3H), 7.31 (dd, J = 7.68, 8.79 Hz, 2H), 7.50 (d, J = 8.79 Hz, 2H), 12.21 (s, 1H); ^{13}C NMR δ 21.1, 21.2, 30.9, 76.0, 101.8, 103.7, 104.2, 113.0 (2C), 121.3, 122.1 (2C), 127.3 (2C), 140.0 (2C), 136.8, 143.1, 143.7, 150.8, 152.3, 157.0, 159.2, 169.2, 169.5; IR (cm^{-1}) 3334, 2922, 2850, 1751, 1601, 1499, 1368, 1190, 1123, 1021; HRFABMS calcd for $C_{25}H_{22}N_2O_6$ $(M + Na)^+$ 469.1376, found 469.1372.

Antibodies. Antibodies specific to PARP, caspase-3, caspase-8, caspase-9, phospho-GSK3α/β (Ser-21/9), Bcl-2, Bcl-xL, and Bax, as well as an α-mouse IgG horseradish peroxidase (HRP) conjugated secondary antibody, were purchased from Cell Signaling Technology (Beverly, MA). Antibodies specific to PI3K, phospho-Akt1/2/3 (Ser-473), Akt, GSK-3 α/β, p27, p21, NF-Kb p65, and GAPDH, as well as an α-rabbit IgG HRP conjugated secondary antibody, were purchased from Santa Cruz Biotechnology (Santa Cruz, CA). Antibodies specific to cyclin D1, cyclin A, and phospho-pRb were purchased from BD Bioscience (San Diego, CA). Anti-p53 antibody was from Oncogene (Cambridge, MA).

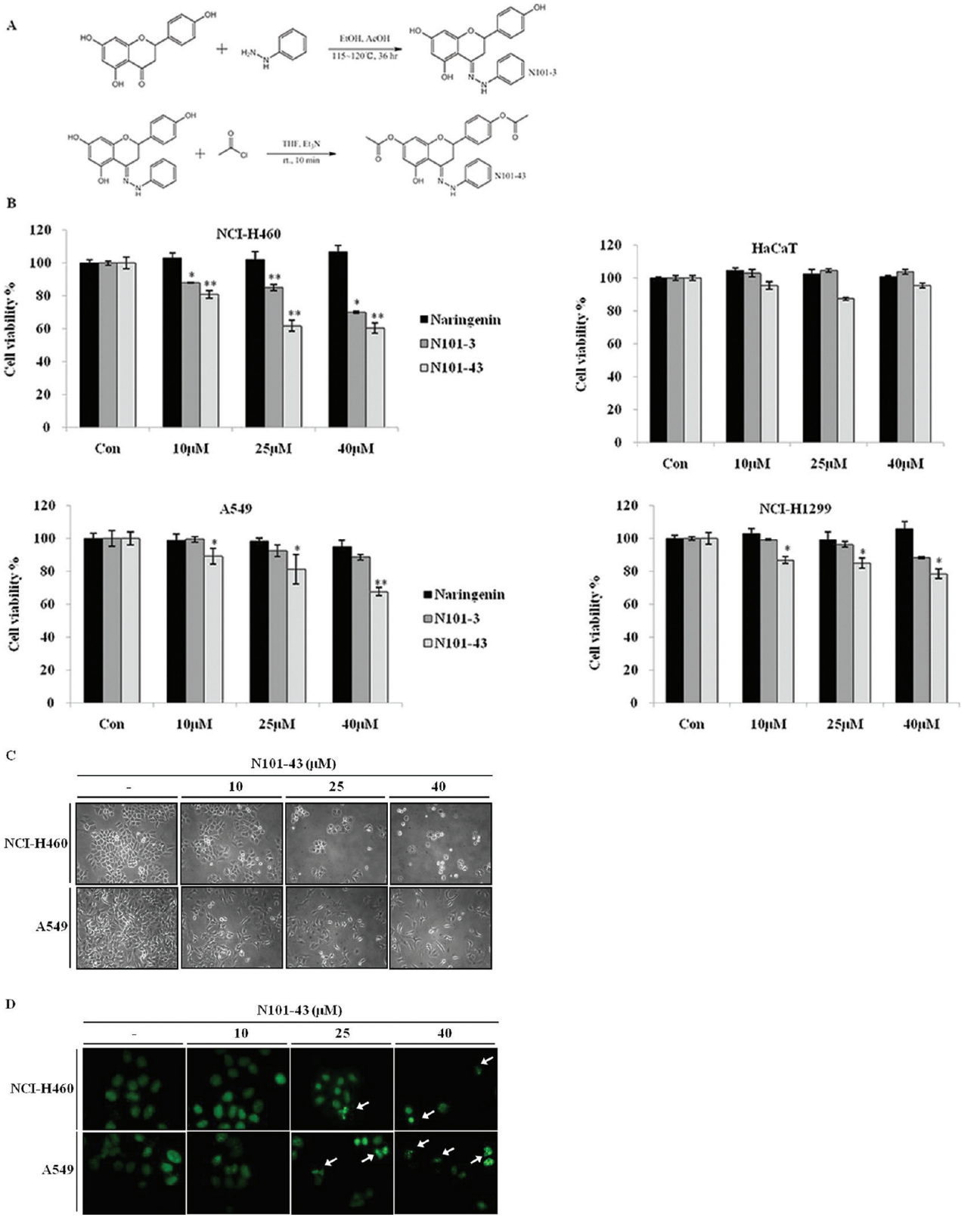

Figure 1. Antiproliferative and apoptotic effects of naringenin and naringenin derivatives in human lung cancer cell lines. (A) Chemical structures of naringenin and the naringenin derivatives 5,7,4′-trihydroxyflavanone *N*-phenyl hydrazone (N101-3) and 5-hydroxy-7,4′-diacetyloxyflavanone-*N*-phenyl hydrazone (N101-43). (B) Cytotoxic effects of naringenin and naringenin derivatives on human lung cancer cell lines (NCI-H460, A549, NCI-H1299) and keratinocytes (HaCaT). Cells were treated with naringenin or naringenin derivatives in complete medium for 24 h before assessment of cell viability by MTS assay. Data are presented as the mean ± standard deviation ($n = 3$). (∗)$p < 0.05$ and (∗∗) $p < 0.005$ versus DMSO treated cells. (C) NCI-H460 or A549 cells cultured in different concentrations of N101-43 for 24 h observed by phase-contrast microscopy (40×) and photographed. (D) Nuclear morphological changes observed by fluorescence microscopy (Hoechst staining, 100×).

Cell Culture. We obtained the NCI-H460, A549, and NCI-H1299 non-small-cell lung cancer cell lines from the American Type Culture Collection (ATCC; Rockville, MD). NCI-H460, A549, and NCI-H1299 cells were cultured in RPMI medium supplemented with heat-inactivated 10% (v/v) fetal bovine serum (FBS; both from Hyclone Laboratories, Logan, UT) and incubated under humidified conditions at 5% CO_2 and 37 °C.

Cell Viability Assays. Cell viability was quantified using an MTS assay (Promega, Madison, WI). Approximately 0.7×10^4 cells were seeded in each well of a 96-well plate containing 100 μL of RPMI supplemented with 10% FBS, penicillin (100 μg/mL), and streptomycin (0.25 μg/mL) for overnight growth. After 20 h, various concentrations of N101-43 were added and incubation was continued for a further 24 h. One hundred microliters of medium was removed and 20 μL of MTS solution (2 mg/mL) added to cells for 30 min−1 h at 37 °C. Optical density was measured at 492 nm using an ELISA reader (Apollo LB 9110, Bertholo, Technologies GmbH, Germany).

siRNA Transfection. siRNA oligonucleotide of p53 and FasL and scrambled siRNA were purchased from ST Pharm. Co., Ltd. (Seoul, Korea). Sequences: p53 oligonucleotide, sense 5′-CACUACAACUACAUGUGUA-3′ and antisense 5′-UACACAUGUAGUUGUAGUG (dTdT)-3′;[33] FasL siRNA, 5′-CUGGGCUGUACUUUGUACATT-3′;[34] scrambled siRNA, sense 5′-CCUACGCCACCAAUUUCGU (dTdT)-3′ and antisense 5′-ACGAAAUUGUGGCGUAGG (dTdT)-3′.[33] Approximately, 6×10^4 cells were seeded in each well of a 6-well plate containing 10% FBS incubated overnight to give 3−40% confluence. Transfection was performed using a TransIT-TKO reagent (Mirus, Milwaukee, WI) to give a final RNA concentration of 50 nM. After 48 h, cells were treated with N101-43 for 24 h and harvested for Western blot analysis.

Western Blot Analysis. N101-43-treated cells were scraped from plate wells and collected by centrifugation (72*g*, 5 min, 4 °C). Cells were then washed with ice-cold phosphate-buffered saline (PBS) and recentrifuged (1890*g*, 5 min, 4 °C). The cell pellets obtained were resuspended and lysed in buffer containing 20 mM Tris (pH 7.4), 200 mM sodium chloride, 1 mM ethylenediaminetetraacetic acid (EDTA), 10 mM β-glycerophosphate, 10 mM sodium pyrophosphate, 0.5% NP-40, 0.05% sodium deoxycholic acid, and protease inhibitor cocktail, and lysates were clarified by centrifugation at 17010*g* for 30 min at 4 °C. Protein concentrations were measured by using Bradford assay (Bio-Rad, Hercules, CA) with a UV spectrophotometer (Biochrom, WPA, Biowave II, U.K.). Cell lysates were mixed with equal volumes of 5× SDS sample buffer, boiled for 5 min, and separated by 10−12% sodium dodecyl sulfate−polyacrylamide gel electrophoresis (SDS-PAGE). After electrophoresis, proteins were transferred to polyvinylidene difluoride (PVDF) membranes (Millipore, Billerica, MA). Membranes were blocked in 5% nonfat dry milk dissolved in PBST (3.2 mM Na_2HPO_4, 0.5 mM KH_2PO_4, 1.3 mM KCl, 135 mM NaCl, 0.05% Tween-20) overnight at 4 °C. Primary antibodies specific to PARP, caspase-3, caspase-8, caspase-9, Bcl-2, Bcl-xL, Bax, phospho-GSK3 (Ser 21/9), PI3K, phospho-Akt1/2/3 (Ser-473), Akt, GSK-3 α/β, p27, p21, cyclin D1, cyclin A, phospho-pRb, and p53 were adsorbed to membranes. HRP-conjugated α-rabbit or α-mouse IgG was used as a secondary antibody. Immune-positive bands were visualized by using Westzol plus Western blot detection system (iNtRON Biotechnology, Sung-Nam, South Korea). All membranes were stripped, reblocked, and reprobed with anti-GAPDH antibody as an internal control to confirm equal protein loading.

Hoechst Staining. Apoptotic nuclear morphology was observed through Hoechst staining. Cells were seeded on coverslips and then cultured in a range of concentrations (0, 10, 25, and 40 μM) of N101-43 for 24 h. Coverslips were washed twice with PBS and fixed with 4% paraformaldehyde for 1 h at room temperature. After three washes in PBS, the cells were stained with Hoechst staining solution at 37 °C; coverslips were then washed with PBS a further three times, dried completely, and mounted on microscope slides with mounting solution. Slides were imaged with fluorescence microscopy.

Cell Cycle Analysis by Flow Cytometry. Approximately 1×10^5 cells were seeded per well of 6-well plates and incubated for 24 h before treatment with various concentrations of N101-43 and a further 24 h of incubation. The cells were then washed, harvested, and fixed with ice-cold 70% ethanol at −20 °C. After fixation, the cells were washed with PBS and stained for 30 min with PBS containing 50 μg/mL PI and 100 μg/mL RNase A. The proportion of apoptotic cells was determined by flow cytometry on a FACScalibur instrument and analyzed with CellQuest software (BD Bioscience). The sub-G1 population indicated apoptosis-associated chromatin degradation.

Flow Cytometry Analysis after Annexin V and PI Staining. Apoptosis was detected by flow cytometry using an Annexin V-FITC Apoptosis Detection Kit (BD Pharmigen). Briefly, 1.5×10^5 cells were seeded per well of 6-well plates and incubated to adhere for overnight. Cells were treated with various concentrations of N101-43 for 24 h, harvested, and washed with PBS, and the cell pellets were resuspended in annexin binding buffer. Cells were double-stained with annexin V-FITC and PI following the manufacturer's instruction. Early apoptosis is defined by annexin V^+/PI^- staining, and late apoptosis is defined by annexin V^+/PI^+ staining as determined by FACS Calibur flow cytometry (Becton Dickinson & Co., Franklin Lakes, NJ) and Cell Quest Pro software.

Reverse-Transcription Polymerase Chain Reaction (RT-PCR) and Real-Time qPCR Analyses. Total RNA was isolated using the Easy-BLUE Total RNA Extraction Kit (iNtRon Biotechnology, Seoul, Korea) according to the manufacturer's instructions. Reverse transcription was performed using M-MuLV reverse transcriptase (New England Biolabs, Beverly, MA). RT-PCR analysis was performed using a PCR thermal cycler Dice instrument (TaKaRa, Otsu, Shiga, Japan) with the following primer sets: FasL, 5′-CAA GAT TGA CCC CGG AAG TA-3 (forward), 5′-GGC CTG TGT CTC CTT GTG AT-3′ (reverse); GAPDH, 5′-TGA TGA CAT CAA GAA GGT GGT-3′ (forward), 5′-TCC TTG GAG GCC ATG TAG GCC-3′ (reverse). GAPDH served as internal control. Real-time quantitative PCR was performed with a relative quantification protocol using the Chromo 4 Real-Time PCR system and iQ SYBR Green Supermix (both from Bio-Rad, Hercules, CA). All target genes were normalized to expression of the housekeeping gene GAPDH. Each sample was run with the following primer sets: FasL, 5′-GCA GCC CTT GAA TTA CCC AT-3′ (forward), 5′-CAG AGG TTG GAC AGG GAA GAA-3′ (reverse); Fas, 5′-TGA AGG ACA TGG CTT AGA AGT G-3′ (forward), 5′-GGT GCA AGG GTC ACA GTG TT-3′ (reverse); GAPDH, 5′-GGC TGC TTT TAA CTC TGG TA-3′ (forward), 5′-TGG AAG ATG GTG ATG GGA TT-3′ (reverse). Fold changes in expression represent the ratio of Fas or FasL expression in NCI-H460 and A549 cells treated with N101-43 to untreated control.

Statistical Analysis. Data presented are the mean ± SD of results from at least three independent experiments. Statistical significance was assessed with Student's *t* test. *, $P < 0.05$, or **, $P < 0.005$, were considered to be statistically significant.

RESULTS

N101-43 Suppresses Cell Proliferation and Induces Apoptotic Bodies in NSCLC. We treated non-small-cell lung cancer-cell lines (NCI-H460, A549, NCI-H1299) and normal keratinocyte cells (HaCaT) with 10−40 μM naringenin or naringenin derivatives (N101-3, N101-43) for 24 h and assessed cell viability by MTS assay. Naringenin and N101-3 had little effect on proliferation in any cell line. However, N101-43 significantly reduced viability much more in NCI-H460 and A549 cells (both p53 +/+) than in NCI-H1299 (p53 −/−) in a dose-dependent

manner (Figure 1B). In contrast, however, the viability of HaCaT cells was very slightly decreased after culture with N101-43 (Figure 1B). These results suggest that N101-43 effectively inhibits the growth of NSCLCs.

We wished to explore N101-43's capacity for growth inhibition more fully. We found that N101-43 suppressed cell growth in NCI-H460 and A549 cell lines, with a more pronounced effect on the former (Figure 1B,C). To determine whether this effect was apoptotic in nature, we cultured NCI-H460 and A549 cells with various concentrations of N101-43 for 24 h, then stained cultures with Hoechst dye and monitored cellular appearance by fluorescence microscopy. Nuclear condensation

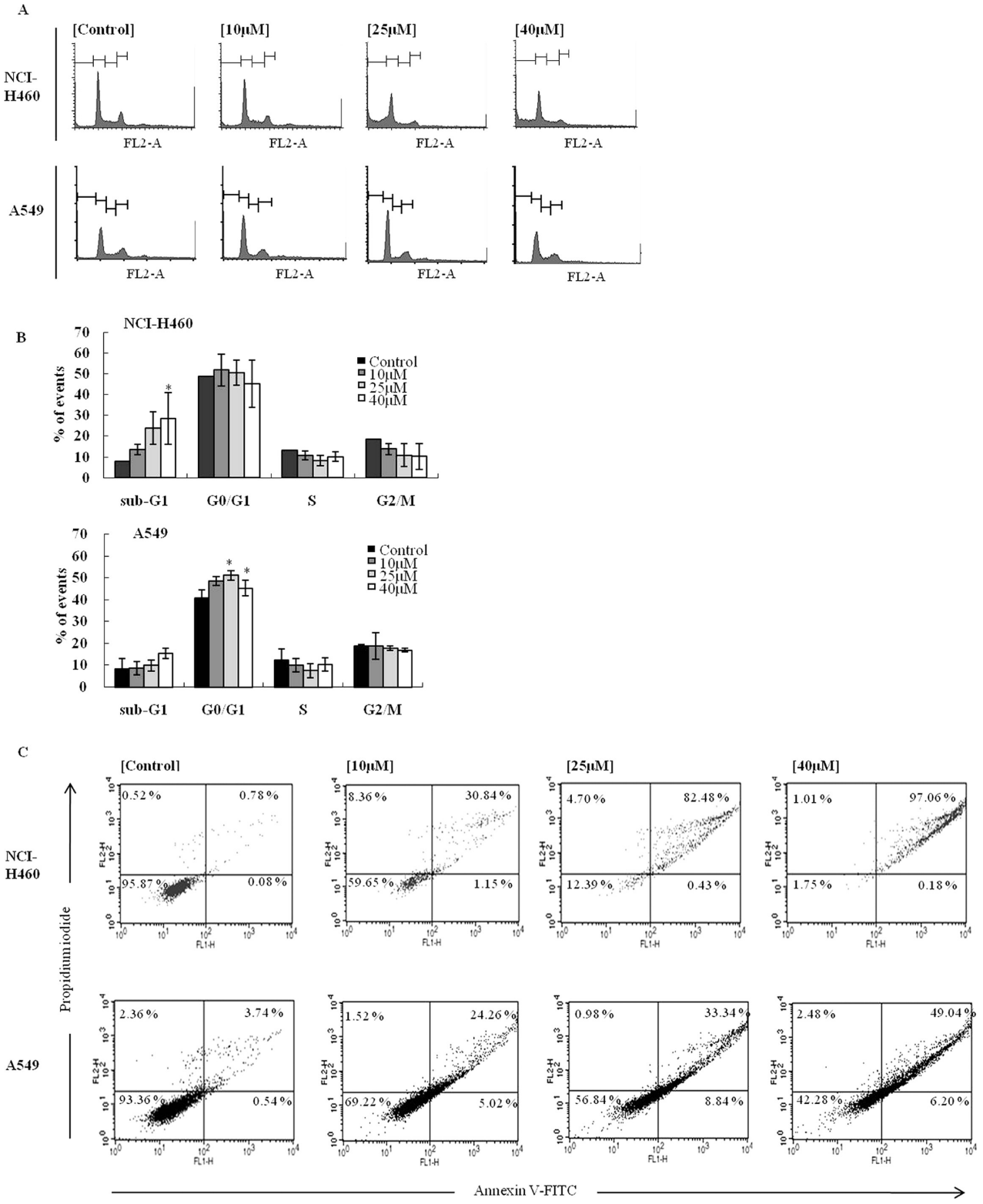

Figure 2. Continued

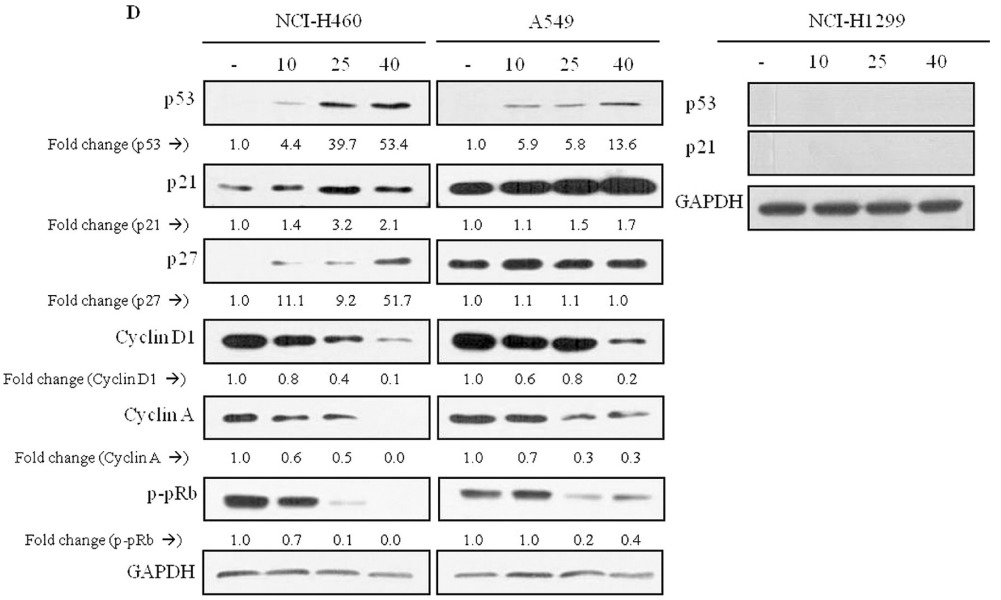

Figure 2. Effects of N101-43 on cell cycle progression in NCI-H460 and A549 cells. Cells were treated with the indicated concentrations of N101-43 for 24 h, fixed with 70% ethanol, and stained with PI; 10000 events were measured per experimental condition by flow cytometry. (A) Representative examples of cell cycle analysis by flow cytometry with PI staining. (∗) $p < 0.05$ versus DMSO treated cells. (B) Flow cytometry analyses of the cell cycle. (C) Flow cytometry analysis after annexin V and PI staining. Apoptosis was detected by flow cytometry using an Annexin V-FITC Apoptosis Detection Kit (BD Pharmigen). Cells were treated with various concentrations of N101-43 for 24 h, harvested, and washed with PBS, and the cell pellets were resuspended in annexin binding buffer. Cells were double-stained with annexin V-FITC and propidium iodide (PI) following the manufacturer's instruction. (D) Expression levels of cell cycle regulators cyclins A and D1, p27, p21, p53, and phospho-pRb detected by Western blot analysis. GAPDH was used as an internal control for sample loading. Densitometric quantification was performed using ImageJ densitometry. The intensity of the control was normalized to 1, and the intensity of each band from N101-43-treated cells is compared to the control. (E) Effect of p53 knockdown on p53 and p21 expressions in NCI-H460 and A549 cells. p53 and p21 were detected by Western blot analysis.

and fragmentation, morphological features of apoptosis, manifested themselves dose-dependently (Figure 1D). These results indicate that N101-43 engendered apoptotic rather than necrotic cell death in NCI-H460 and A549 cells.

N101-43 Induces Cell Cycle Arrest and Up-regulates Cell Cycle Related Proteins. Flow cytometry analyses revealed enhanced apoptosis in NCI-H460 cells treated with N101-43 for 24 h (Figure 2A), concomitant with a dose-dependent increase from 7.81 to 28.45% in the proportion of the NCI-H460 cell population at sub-G_1 phase; there was no significant alteration in the accumulation of cells in G_0/G_1 phase (from 48.86 to 45.18%) after 24 h of treatment (Figure 2B). A549 cells demonstrated a similar response to the compound: the proportion of cells at sub-G_1 phase was increased from 8.16 to 15.39% by treatment with high concentrations of N101-43 ($p = 0.079$), and the percentage of cells at G_0/G_1 phase rose from 40 to 45−50%. Our findings therefore suggested that N101-43 could arrest progression in the sub-G1 or G_0/G_1 cell cycle in NSCLCs. To confirm apoptosis, flow cytometry was performed using an Annexin V-FITC Apoptosis Detection Kit. N101-43 induced late apoptosis defined by annexin V^+/PI^+ staining in NCI-H460 and A549 cell lines, with a more pronounced effect on the former (Figure 2C).

To confirm our observation that N101-43 induced cell cycle arrest, we performed immunoblot analyses on cell cycle regulated proteins. As illustrated in Figure 2D, expression of cyclin D1, cyclin A, and phospho-pRb was down-regulated in N101-43-treated NCI-H460 and A549 cell lines. In contrast, expression of p21 and p53, which tightly control entry into G_1, was elevated in both cell lines; p27 was up-regulated in N101-43-treated NCI-H460, whereas N101-43 treatment slightly up-regulated p27 in A549 cells.

We next assayed NCI-H1299 (p53 −/−) lung cancer cells to probe whether N101-43 might induce p21 and p53 independently. As shown in Figure 2D (right panel), neither p53 nor p21 expression was detected in these cells. To compare drug response in NSCLC (NCI H460 and A549) versus NSCLC with p53 knockdown, we transfected with p53 siRNA, and alternative expression of p53 and p21 induced by N101-43 was examined by Western blotting (Figure 2E). p21, a CDK inhibitor that induces G1 arrest, was inhibited in NCI-H460 and A549 cells treated with p53 siRNA (Figure 2E), indicating that N101-43-induced G1 arrest is p53-dependent. Therefore, it was assumed that p53-dependent and/or other pathways can be involved in the inhibiting effect of N101-43 on NSCLC cell growth. These results show that the NSCLC tumor-killing effect of N101-43 is primarily mediated via the p53-dependent apoptotic pathway. Taken together, these findings imply that N101-43 imposes cell cycle arrest at sub-G_1 phase and/or G_0/G_1 in NCI-H460 and A549 cells via G1/S cyclin down-regulation and p53-dependent p21 up-regulation.

N101-43 Induces Pro-apoptotic Signaling Pathways. Caspases play crucial roles in apoptosis through their proteolysis of specific targets. To establish more concretely N101-43's manner of inducing apoptosis, we assessed caspase activation as well as expression of pro- and anti-apoptotic proteins in NCI-H460 and A549 cells treated with N101-43. Treatment with N101-43 significantly induced cleavage of caspase-3 and -8 in either cell line (Figure 3A). We further queried the effect of N101-43 on PARP, determining that its processing likewise rose dose-dependently (Figure 3A). A pan-caspase inhibitor, Z-VAD-fmk, was used to confirm caspase activation. Z-VAD-fmk inhibited

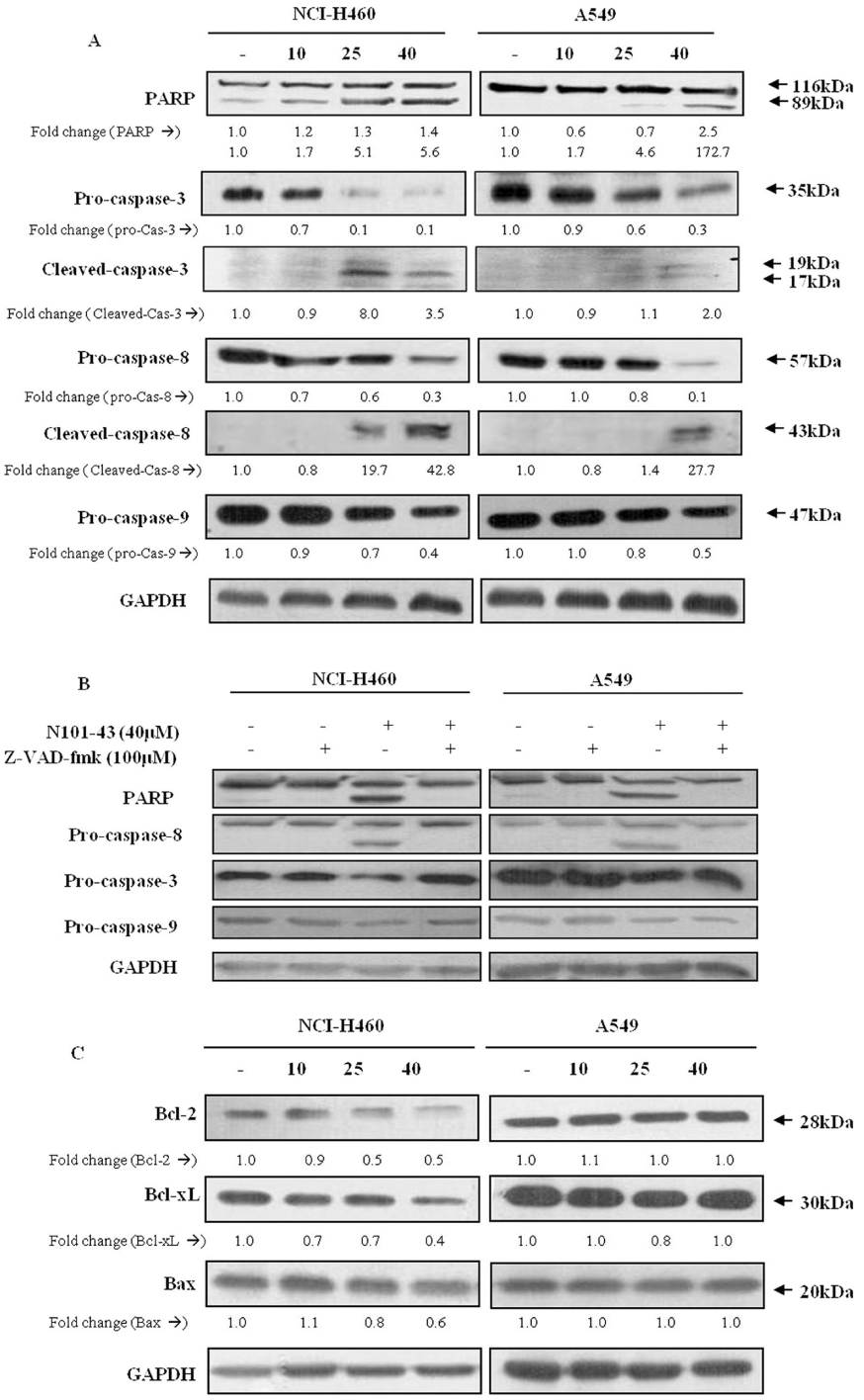

Figure 3. Effects of N101-43 on expression of apoptotic factors in NCI-H460 and A549 cell lines. Cells were treated with different concentrations of N101-43 for 24 h. (A) Processing of caspase-3, caspase-8, caspase-9, and PARP and (B) inhibitory effect of a pan-caspase inhibitor, Z-VAD-fmk, on expression of caspase-3, caspase-8, caspase-9, and PARP detected by Western blot analyses. Z-VAD-fmk (100 μM) was pretreated for 2 h, and then N101-43 (40 μM) was treated for 24 h into cells. (C) Expression levels of Bax, Bcl-2, and Bcl-xL detected by Western blot analyses. The intensity of the control was normalized to 1, and the intensity of each band from N101-43-treated cells is compared to the control.

N101-43-induced cleavages of PARP and pro-casoase-8 in both NSCLC cells, and the decreased levels of pro-caspase-3 and -9 were recovered in N101-43-treated NCI-H460 cells (Figure 3B).

The mitochondrial, or intrinsic, apoptosis pathway comprises pro- and anti-apoptotic members including Bcl-2 family proteins.[35] We investigated N101-43's capacity to evoke intrinsic apoptosis by Western blotting. As shown in Figure 3C, levels of pro-apoptotic Bax were unchanged by N101-43 treatment, whereas the levels of pro-survival Bcl-2 and Bcl-xL were markedly reduced, in NCI-H460 cells. In A549, in contrast, no such alterations in protein expression occurred subsequent to N101-43 treatment, but caspase-3 was activated. These results suggest that extrinsic signaling appears to predominate in A549 cells,

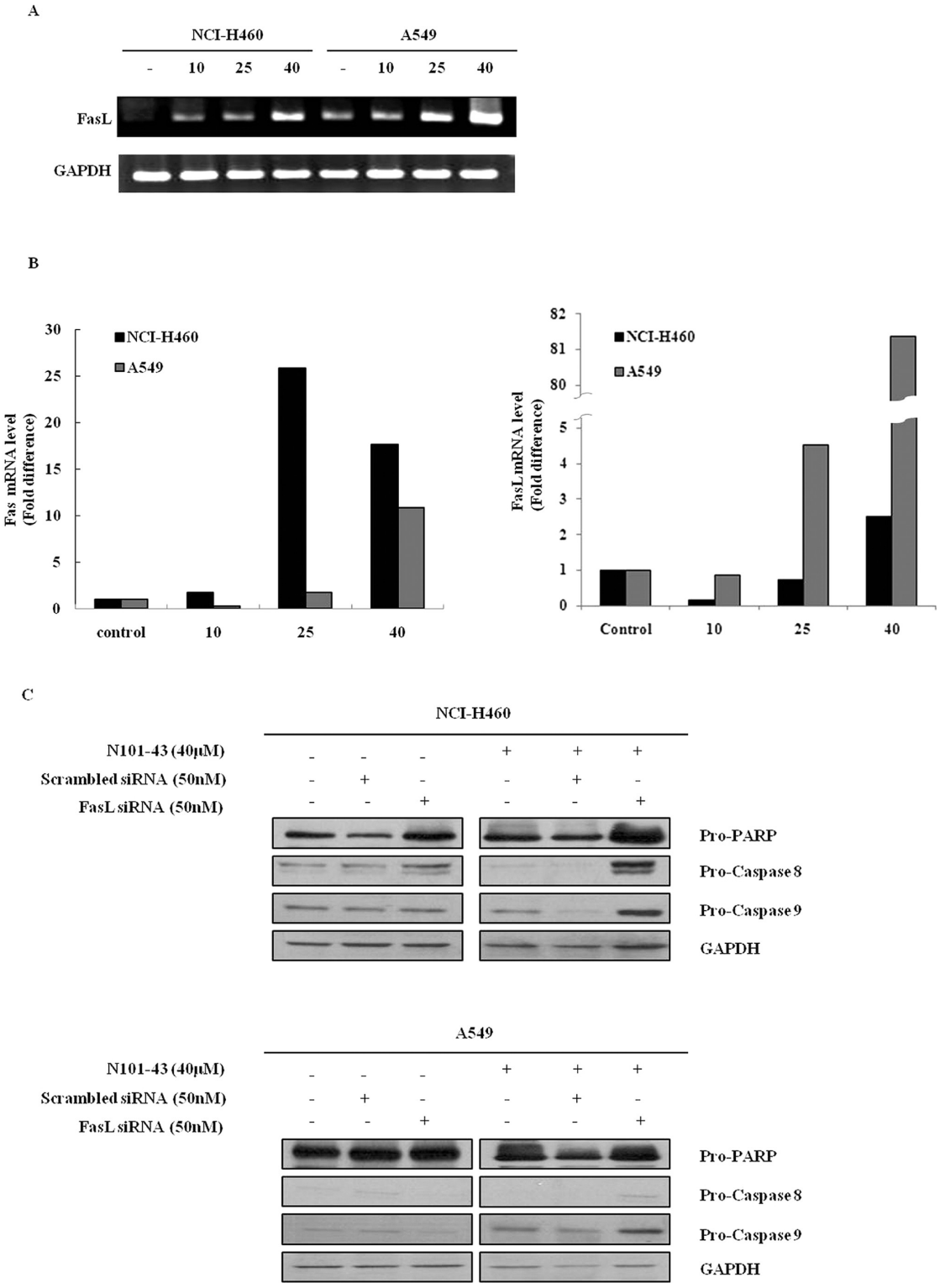

Figure 4. Effects of N101-43 on Fas/FasL expression in NCI-H460 and A549 cells. (A) FasL gene induction in NCI-H460 and A549 cells treated with N101-43. FasL expression was analyzed by RT-PCR; the PCR products depicted were amplified for 38 cycles. (B) Expression levels of Fas and FasL mRNA measured by real-time quantitative PCR. GAPDH was used as an internal control. (C) Effect of FasL knockdown on expressions of PARP and caspases in NCI-H460 and A549 cells. Expressions of PARP and caspases were detected by Western blot analysis.

whereas intrinsic and extrinsic apoptotic signaling likely contribute to N101-43's cytotoxicity in NCI-H460 cells.

To investigate the extrinsic signaling, RT-PCR and real-time PCR analyses were performed to investigate modulation of Fas expression: Fas and FasL transcription were increased dose-dependently by N101-43 in both NCI-H460 and A549 cells, with Fas mRNA substantially increased in NCI-H460 cells (Figure 4B, left panel) and FasL mRNA levels rising in A549 cells (Figure 4A,B).

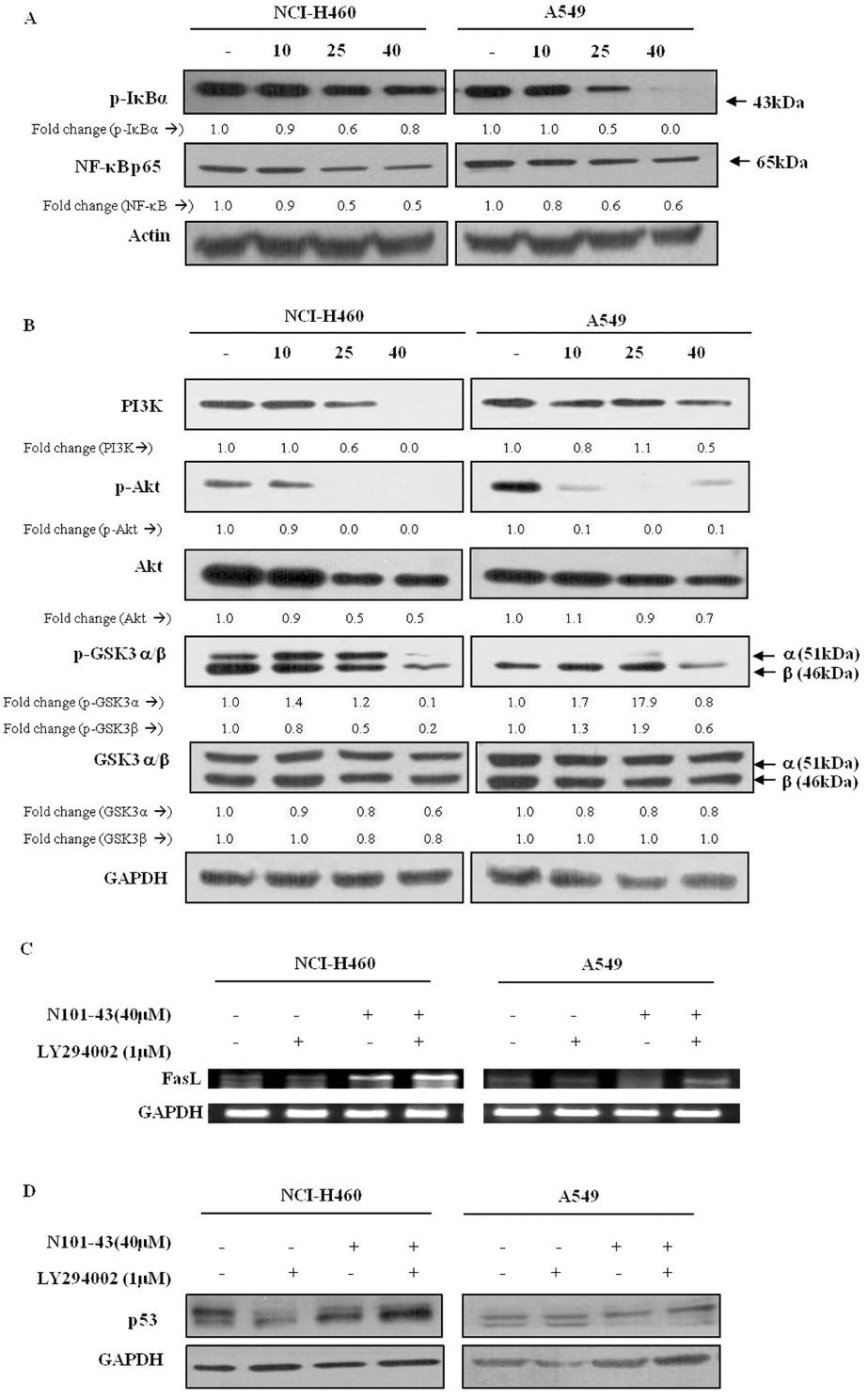

Figure 5. Inhibitory effects of N101-43 on PI3K/AKT cell survival factors and IκB phosphorylation in NCI-H460 and A549 cell lines. Cells were treated with different concentrations of N101-43 for 24 h. (A) IκB phosphorylation and (B) expression levels of PI3K, phospho-Akt, Akt, phospho-GSK3α/β, and GSK3 α/β detected by Western blot analyses. The intensity of the control was normalized to 1, and the intensity of each band from N101-43-treated cells is compared to the control. (C, D) Effects of PI3K inhibitor LY294002 on N101-43-induced FasL and p53 expression and p53 detected by RT-PCR (C) and Western blot analyses, respectively. LY294002 (1 μM) was pretreated for 1 h, and then N101-43 (40 μM) was treated for 24 h into cells.

However, no significant changes in FADD levels were observed (data not shown). These results suggest that extrinsic apoptotic signaling mediated via enhanced FasL expression appears to predominate in A549 cells. To compare drug response in NSCLC (NCI H460 and A549) versus NSCLC with p53 knockdown, we transfected with FasL siRNA, and alternative expression of PARP and caspases induced by N101-43 was examined by Western blotting (Figure 4C). The expression levels of precursor

caspase-8 and -9 and PARP were enhanced in N101-43-treated cells by FasL knockdown (Figure 4C), assuming that N101-43-induced cleavages of PARP and caspases are primarily FasL-dependent. Collectively, these results show that the NSCLC tumor-killing effect of N101-43 is primarily mediated via the FasL-dependent apoptotic pathway.

As a major cell survival signal, nuclear factor-κB (NF-κB) participates in multiple steps in cancer cells' resistance to chemical and radiation therapies. Recent studies with animal models and cell culture systems have established links between NF-κB and lung carcinogenesis, highlighting its significance as a target in lung cancer treatment and chemoprevention.[36] We therefore probed the possibility that N101-43 might inhibit NF-κB in NCI-H460 and A549 cell lines. Indeed, N101-43 inhibited the phosphorylation of IκB, an upstream mediator of NF-κB function, and thus p65 localization into nuclear was also inhibited in cells activated by N101-43 (Figure 5A), supporting the involvement of NF-κB inactivation in N101-43-induced apoptosis. Our findings therefore suggested that N101-43 initially stimulates the activation of Fas and FasL, in the extrinsic apoptosis module, with the consequence of downstream activation of caspase-3 and -8 and PARP through inhibition of NF-κB in lung cancer cell lines.

It is known that PI3K and its downstream substrate Akt also have a hand in apoptosis.[37,38] We examined the expression of these proteins, identifying dose-dependent reductions in PI3K and phospho-Akt in both NCI-H460 and A549 cell lines. phospho-GSK α/β also diminished upon N101-43 stimulation of NCI-H460 cells; nevertheless, no significant change in total GSK α/β protein levels was observed, indicating that N101-43 does not affect overall GSK α/β protein stability. We examined whether or not PI3K inhibition can enhance FasL and p53 expression in NCI-H460 and A549 cell lines, where N101-43 suppressed cell growth in NCI-H460 and A549 cell lines, with a more pronounced effect on the former (Figure 1B,C). PI3K inhibitor LY294002 also showed a more pronounced effect on N101-43-induced FasL and p53 expression in NCI-H460 as in Figure 5D. These results indicate that N101-43 appears to promote programmed cell death through the PI3K/Akt pathway in lung cancer cell lines.

DISCUSSION

Plant extracts demonstrate significant potential as anticancer therapeutic agents due to their ability to inhibit tumor growth, angiogenesis, and metastasis with few side effects.[39] Much of this activity appears to stem from flavonoids, which are principal components of many such extracts and demonstrate the capacity to inactivate carcinogens, inhibit angiogenesis, and halt cell proliferation or promote apoptosis.[40] Naringenin is a flavonoid abundant in citrus fruits, especially their peels and rinds, and has been suggested to exhibit antiproliferative effects against human tumor cells. Here we endeavored to investigate the effects of the naringenin derivative N101-43 on lung cancer cell development.

We first investigated the antiproliferative effects of N101-43 on the NSCLC cell lines NCI-H460 (p53 +/+), A549 (p53 +/+), and NCI-H1299 (p53 −/−). N101-43 was cytotoxic to NCI-H460 and A549 cells and less so to NCI-H1299; HaCaT keratinocyte control cells were not affected by the compound. N101-43 therefore appeared to reduce cancer cell growth with minimal collateral damage.

We observed cell cycle arrest when cells were cultured with N101-43. Characterization of this effect demonstrated that expression levels of cell cycle regulators were modulated by N101-43 treatment; arrest appeared to occur at sub-G_1 or G_0/G_1 phase.

Apoptosis is a cell suicide mechanism frequently dysregulated in oncogenesis. Caspase cascades operate in both intrinsic and extrinsic apoptosis. Intrinsic (mitochondrial) programmed cell death often involves an increase in mitochondrial membrane permeability, coupled to release of cytochrome *c*, whereas the extrinsic (death receptor) pathway involves oligomerization of death receptors and recruitment of Fas-associated death domain protein (FADD); activation of caspase-8 occurs downstream of these signals and stimulates cleavage of other caspases such as caspase-3 and PARP.[41] To characterize the apoptotic mechanisms induced by N101-43, we assessed expression of pro- and anti-apoptotic proteins, finding that cleavage of caspase-3, -8, and -9 and PARP was promoted by N101-43 treatment.

The PI3K/Akt signaling pathway is influential in the regulation of cell survival, as activation of anti-apoptotic downstream effectors,[42] phosphorylation-dependent inhibition of pro-apoptotic signals of such as BAD protein, caspase-9, and the family of Forkhead transcription factors.[43−45] Recent works revealed that Akt inhibition results in the up-regulation of FasL expression in vascular smooth muscle cells (VSMC) and HeLa cells.[46,47] Down-regulation of Akt leads to decrease in phosphorylation of the endogenous Forkhead and its location to the nucleus. It impairs the induction of FasL promoter.[45] In addition, Akt promotes cell survival via activation of NF-κB.[48] NF-κB enhances cell survival and participates significantly in cancer cells' acquisition of resistance to chemical or radiation therapy.[36] As such, NF-κB is an important target for lung cancer treatment and chemoprevention. It has been reported that p53 binds directly to a promoter of *PIK3CA*, which encodes the catalytic subunit of PI3K, and inhibits its activity, whereas inactivation of p53 and subsequent up-regulation of *PIK3CA* may contribute to the pathophysiology of cancer.[49] Our results demonstrated that N101-43 induced p53 expression and inhibited NF-κB as well as PI3K/Akt signaling in lung cancer cells. These data suggest that the major pathways of apoptosis induced by treatment with N101-43 are NF-κB and PI3K/Akt dependent. Because we need more compounds and their biological data to obtain the relationships between the different structures and their biological activities, the current data are not enough for us to predict a structure−activity relationship (SAR). This remains for further study.

In summary, we demonstrate that the naringenin derivative N101-43 induces apoptosis through the Fas (extrinsic) death receptor, accompanied by processing of caspase-8, -3, and -9 and PARP and inhibition of PI3K/Akt signaling, in NCI-460 and A549 cells. N101-43 therefore displays promise as a pro-apoptotic factor that may benefit NSCLC therapy.

AUTHOR INFORMATION

Corresponding Author

*Postal address: Department of Bioscience and Biotechnology, Bio/Molecular Informatics Center, Konkuk University, Hwayang-dong 1, Gwangjin-gu, Seoul 143-701, Republic of Korea. Fax: +82-2-444-4218. Phone: +82-2-450-4119. E-mail: ydy4218@konkuk.ac.kr.

Author Contributions

‖These authors contributed equally to this work.

Funding Sources

This research was supported by a Korea Research Foundation (KRF) grant funded by the Korean government (MEST 2010-0019306, 2009-0072028). D.-Y.Y. is partially supported by the Priority Research Centers Program (2009-0093824) and the National R&D Program for Cancer Control, Ministry for Health, Welfare, and Family aAffairs, Republic of Korea (0920080).

■ ACKNOWLEDGMENT

The synthetic naringenin derivative N101-43 was the generous gift of Professor K. Y. Jung, Department of Biochemical Engineering, Gangneung-Wonju National University (Gangneung, Korea).

■ ABBREVIATIONS USED

NSCLC, non-small-cell lung cancer; DMSO, dimethyl sulfoxide; N101-3, 5,7,4′-trihydroxy flavanone *N*-phenyl hydrazone; N101-43, 5-hydroxy-7,4′-diacetyloxyflavanone-*N*-phenyl hydrazone-PARP, poly(ADP-ribose) polymerase; PBS, phosphate-buffered saline; PI, propidium iodide; PVDF, polyvinylidene difluoride; PI3K, phosphatidylinositol 3-kinase; SDS-PAGE, sodium dodecyl sulfate−polyacrylamide gel electrophoresis.

■ REFERENCES

(1) Jemal, A.; Thomas, A.; Murray, T.; Thun, M. Cancer statistics. *CA Cancer J. Clin.* **2002**, *52*, 23–47.

(2) Lee, E. R.; Kang, Y. J.; Choi, H. Y.; Kang, G. H.; Kim, J. H.; Kim, B. W.; Han, Y. S.; Nah, S. Y.; Paik, H. D.; Park, Y. S.; Cho, S. G. Induction of apoptotic cell death by synthetic naringenin derivatives in human lung epithelial carcinoma A549 cells. *Biol. Pharm. Bull.* **2007**, *30*, 2394–2398.

(3) Herbst, R. S.; Heymach, J. V.; Lippman, S. M. Lung cancer. *N. Engl. J. Med.* **2008**, *359*, 1367–1380.

(4) Hengartner, M. O. The biochemistry of apoptosis. *Nature* **2000**, *407*, 770–776.

(5) Hanahan, D.; Weinberg, R. A. The hallmarks of cancer. *Cell* **2000**, *100*, 57–70.

(6) Evan, G. I.; Vousden, K. H. Proliferation, cell cycle and apoptosis in cancer. *Nature* **2001**, *411*, 342–348.

(7) Ashkenazi, A.; Dixit, V. M. Death receptors: signaling and modulation. *Science* **1998**, *281*, 1305–1308.

(8) Thornberry, N. A.; Rano, T. A.; Peterson, E. P.; Rasper, D. M.; Timkey, T.; Garcia-Calvo, M.; Houtzager, V. M.; Nordstrom, P. A.; Roy, S.; Vaillancourt, J. P.; Chapman, K. T.; Nicholson, D. W. A combinatorial approach defines specificities of members of the caspase family and granzyme B. Functional relationships established for key mediators of apoptosis. *J. Biol. Chem.* **1997**, *272*, 17907–17911.

(9) Walczak, H.; Krammer, P. H. The CD95 (APO-1/Fas) and the TRAIL (APO-2L) apoptosis systems. *Exp. Cell Res.* **2000**, *256*, 58–66.

(10) Fulda, S.; Debatin, K. M. Extrinsic versus intrinsic apoptosis pathways in anticancer chemotherapy. *Oncogene* **2006**, *25*, 4798–4811.

(11) Kischkel, F. C.; Hellbardt, S.; Behrmann, I.; Germer, M.; Pawlita, M.; Krammer, P. H.; Peter, M. E. Cytotoxicity-dependent APO-1 (Fas/CD95)-associated proteins form a death-inducing signaling complex (DISC) with the receptor. *EMBO J.* **1995**, *14*, 5579–5588.

(12) Scaffidi, C.; Fulda, S.; Srinivasan, A.; Friesen, C.; Li, F.; Tomaselli, K. J.; Debatin, K. M.; Krammer, P. H.; Peter, M. E. Two CD95 (APO-1/Fas) signaling pathways. *EMBO J.* **1998**, *17*, 1675–1687.

(13) Green, D. R.; Kroemer, G. The pathophysiology of mitochondrial cell death. *Science* **2004**, *305*, 626–629.

(14) Chan, T. O.; Rittenhouse, S. E.; Tsichlis, P. N. AKT/PKB and other D3 phosphoinositide-regulated kinases: kinase activation by phosphoinositide-dependent phosphorylation. *Annu. Rev. Biochem.* **1999**, *68*, 965–1014.

(15) Brunet, A.; Datta, S. R.; Greenberg, M. E. Transcription-dependent and -independent control of neuronal survival by the PI3K-Akt signaling pathway. *Curr. Opin. Neurobiol.* **2001**, *11*, 297–305.

(16) Cross, D. A.; Alessi, D. R.; Cohen, P.; Andjelkovich, M.; Hemmings, B. A. Inhibition of glycogen synthase kinase-3 by insulin mediated by protein kinase B. *Nature* **1995**, *378*, 785–789.

(17) Woodgett, J. R. Molecular cloning and expression of glycogen synthase kinase-3/factor A. *EMBO J.* **1990**, *9*, 2431–2438.

(18) Frame, S.; Cohen, P.; Biondi, R. M. A common phosphate binding site explains the unique substrate specificity of GSK3 and its inactivation by phosphorylation. *Mol. Cell* **2001**, *7*, 1321–1327.

(19) Fang, X.; Yu, S. X.; Lu, Y.; Bast, R. C., Jr.; Woodgett, J. R.; Mills, G. B. Phosphorylation and inactivation of glycogen synthase kinase 3 by protein kinase A. *Proc. Natl. Acad. Sci. U.S.A.* **2000**, *97*, 11960–11965.

(20) Goode, N.; Hughes, K.; Woodgett, J. R.; Parker, P. J. Differential regulation of glycogen synthase kinase-3 β by protein kinase C isotypes. *J. Biol. Chem.* **1992**, *267*, 16878–16882.

(21) Aparicio, I. M.; Garcia-Herreros, M.; Fair, T.; Lonergan, P. Identification and regulation of glycogen synthase kinase-3 during bovine embryo development. *Reproduction* **2010**, *140*, 83–92.

(22) Galluzzo, P.; Marino, M. Nutritional flavonoids impact on nuclear and extranuclear estrogen receptor activities. *Genes Nutr.* **2006**, *1*, 161–176.

(23) Dixon, R. A.; Steele, C. L. Flavonoids and isoflavonoids − a gold mine for metabolic engineering. *Trends Plant Sci.* **1999**, *4*, 394–400.

(24) Bors, W.; Michel, C.; Stettmaier, K. Antioxidant effects of flavonoids. *Biofactors* **1997**, *6*, 399–402.

(25) Heijnen, C. G.; Haenen, G. R.; Oostveen, R. M.; Stalpers, E. M.; Bast, A. Protection of flavonoids against lipid peroxidation: the structure activity relationship revisited. *Free Radical Res.* **2002**, *36*, 575–581.

(26) Manach, C.; Scalbert, A.; Morand, C.; Remesy, C.; Jimenez, L. Polyphenols: food sources and bioavailability. *Am. J. Clin. Nutr.* **2004**, *79*, 727–747.

(27) Jin, C. Y.; Park, C.; Hwang, H. J.; Kim, G. Y.; Choi, B. T.; Kim, W. J.; Choi, Y. H. Naringenin up-regulates the expression of death receptor 5 and enhances TRAIL-induced apoptosis in human lung cancer A549 cells. *Mol. Nutr. Food Res.* **2011**, *55*, 300–309.

(28) Lee, J. H.; Park, C. H.; Jung, K. C.; Rhee, H. S.; Yang, C. H. Negative regulation of β-catenin/Tcf signaling by naringenin in AGS gastric cancer cell. *Biochem. Biophys. Res. Commun.* **2005**, *335*, 771–776.

(29) Park, J. H.; Jin, C. Y.; Lee, B. K.; Kim, G. Y.; Choi, Y. H.; Jeong, Y. K. Naringenin induces apoptosis through downregulation of Akt and caspase-3 activation in human leukemia THP-1 cells. *Food Chem. Toxicol.* **2008**, *46*, 3684–3690.

(30) Sabarinathan, D.; Mahalakshmi, P.; Vanisree, A. J. Naringenin promote apoptosis in cerebrally implanted C6 glioma cells. *Mol. Cell. Biochem.* **2010**, *345*, 215–222.

(31) Kanno, S.; Tomizawa, A.; Ohtake, T.; Koiwai, K.; Ujibe, M.; Ishikawa, M. Naringenin-induced apoptosis via activation of NF-κB and necrosis involving the loss of ATP in human promyeloleukemia HL-60 cells. *Toxicol. Lett.* **2006**, *166*, 131–139.

(32) Lee, E. J.; Kim, D. I.; Kim, W. J.; Moon, S. K. Naringin inhibits matrix metalloproteinase-9 expression and AKT phosphorylation in tumor necrosis factor-α-induced vascular smooth muscle cells. *Mol. Nutr. Food Res.* **2009**, *53*, 1582–1591.

(33) Lim, S. C.; Duong, H. Q.; Choi, J. E.; Parajuli, K. R.; Kang, H. S.; Han, S. I. Implication of PI3K-dependent HSP27 and p53 expression in mild heat shock-triggered switch of metabolic stress-induced necrosis to apoptosis in A549 cells. *Int. J. Oncol.* **2010**, *36*, 387–393.

(34) Ji, J.; Wernli, M.; Mielgo, A.; Buechner, S. A.; Erb, P. Fas-ligand gene silencing in basal cell carcinoma tissue with small interfering RNA. *Gene Ther.* **2005**, *12*, 678–684.

(35) Boise, L. H.; Gonzalez-Garcia, M.; Postema, C. E.; Ding, L.; Lindsten, T.; Turka, L. A.; Mao, X.; Nunez, G.; Thompson, C. B. bcl-x, a bcl-2-related gene that functions as a dominant regulator of apoptotic cell death. *Cell* **1993**, *74*, 597–608.

(36) Chen, W.; Li, Z.; Bai, L.; Lin, Y. NF-κB in lung cancer, a carcinogenesis mediator and a prevention and therapy target. *Front. Biosci.* **2011**, *16*, 1172–1185.

(37) Franke, T. F.; Yang, S. I.; Chan, T. O.; Datta, K.; Kazlauskas, A.; Morrison, D. K.; Kaplan, D. R.; Tsichlis, P. N. The protein kinase encoded by the Akt proto-oncogene is a target of the PDGF-activated phosphatidylinositol 3-kinase. *Cell* **1995**, *81*, 727–736.

(38) Kulik, G.; Klippel, A.; Weber, M. J. Antiapoptotic signalling by the insulin-like growth factor I receptor, phosphatidylinositol 3-kinase, and Akt. *Mol. Cell. Biol.* **1997**, *17*, 1595–1606.

(39) Cragg, G. M.; Newman, D. J.; Snader, K. M. Natural products in drug discovery and development. *J. Nat. Prod.* **1997**, *60*, 52–60.

(40) Kandaswami, C.; Lee, L. T.; Lee, P. P.; Hwang, J. J.; Ke, F. C.; Huang, Y. T.; Lee, M. T. The antitumor activities of flavonoids. *In Vivo* **2005**, *19*, 895–909.

(41) Green, D. R. Apoptotic pathways: paper wraps stone blunts scissors. *Cell* **2000**, *102*, 1–4.

(42) Datta, S. R.; Brunet, A.; Greenberg, M. E. Cellular survival: a play in three Akts. *Genes Dev.* **1999**, *13*, 2905–2927.

(43) Pastorino, J. G.; Tafani, M.; Farber, J. L. Tumor necrosis factor induces phosphorylation and translocation of BAD through a phosphatidylinositide-3-OH kinase-dependent pathway. *J. Biol. Chem.* **1999**, *274*, 19411–19416.

(44) Brunet, A.; Bonni, A.; Zigmond, M. J.; Lin, M. Z.; Juo, P.; Hu, L. S.; Anderson, M. J.; Arden, K. C.; Blenis, J.; Greenberg, M. E. Akt promotes cell survival by phosphorylating and inhibiting a Forkhead transcription factor. *Cell* **1999**, *96*, 857–868.

(45) Ciechomska, I.; Pyrzynska, B.; Kazmierczak, P.; Kaminska, B. Inhibition of Akt kinase signalling and activation of Forkhead are indispensable for upregulation of FasL expression in apoptosis of glioma cells. *Oncogene* **2003**, *22*, 7617–7627.

(46) Suhara, T.; Kim, H. S.; Kirshenbaum, L. A.; Walsh, K. Suppression of Akt signaling induces Fas ligand expression: involvement of caspase and Jun kinase activation in Akt-mediated Fas ligand regulation. *Mol. Cell. Biol.* **2002**, *22*, 680–691.

(47) Uriarte, S. M.; Joshi-Barve, S.; Song, Z.; Sahoo, R.; Gobejishvili, L.; Jala, V. R.; Haribabu, B.; McClain, C.; Barve, S. Akt inhibition upregulates FasL, downregulates c-FLIPs and induces caspase-8-dependent cell death in Jurkat T lymphocytes. *Cell Death Differ.* **2005**, *12*, 233–242.

(48) Madrid, L. V.; Mayo, M. W.; Reuther, J. Y.; Baldwin, A. S., Jr. Akt stimulates the transactivation potential of the RelA/p65 subunit of NF-κB through utilization of the IκB kinase and activation of the mitogen-activated protein kinase p38. *J. Biol. Chem.* **2001**, *276*, 18934–18940.

(49) Astanehe, A.; Arenillas, D.; Wasserman, W. W.; Leung, P. C.; Dunn, S. E.; Davies, B. R.; Mills, G. B.; Auersperg, N. Mechanisms underlying p53 regulation of PIK3CA transcription in ovarian surface epithelium and in ovarian cancer. *J. Cell. Sci.* **2008**, *121*, 664–674.